026 TIRE A PART REPRINT No. 41/70

PROJECT PROJET D95-10-42

35(D)-95-10-42

WATER VAPOR DISTRIBUTION IN THE LOWER STRATOSPHERE OVER NORTH AND SOUTH AMERICA

11 11a

D. McKinnon and H.W. Morewood

30 Vol 27 No 3
30a p 483-493
30b May 70
30c J of Atmospheric Sciences

0911
09a9

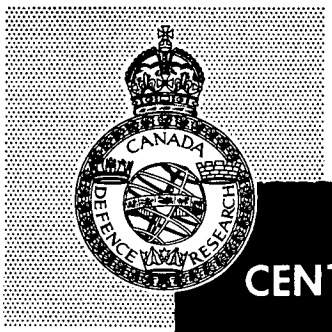

02c

CENTRE DE RECHERCHES POUR LA DÉFENSE
DEFENCE RESEARCH ESTABLISHMENT
VALCARTIER

DEFENCE RESEARCH BOARD

CONSEIL DE RECHERCHES POUR LA DÉFENSE

02d (Québec) Canada

46 May mai 1970

Reprinted from JOURNAL OF ATMOSPHERIC SCIENCES, Vol. 27, No. 3, May 1970, pp. 483–493
American Meteorological Society
Printed in U. S. A.

Water Vapor Distribution in the Lower Stratosphere over North and South America

D. MCKINNON AND H. W. MOREWOOD

Defence Research Establishment Valcartier, Quebec, P. Q., Canada

(Manuscript submitted 8 September 1969, in revised form 18 December 1969)

ABSTRACT

Water vapor concentrations in the upper troposphere and lower stratosphere from 70N to 40S over North and South America were deduced from solar spectra recorded on 56 flights of a high flying jet aircraft. Ambient concentrations between 10.7 and 18.3 km declined with altitude at all latitudes to a minimum at about 2 km above the local tropopause, and remained nearly constant thereafter to 18.3 km. Although seasonal variance was pronounced in the troposphere over New Mexico, changes of only a few per cent were observed in the lower stratosphere, assuming uniform mixing from 17.7 km to the top of the atmosphere. The mean latitudinal distribution of water vapor in the lower stratosphere measured during the Northern Hemispheric winter of 1967–68 showed a maximum concentration of 1.75 mg kg^{-1} at 65N and a progressive decline to a minimum of 1.25 mg kg^{-1} near 30S. Intermediate minima and maxima were also observed at 25N and 10N, respectively.

1. Introduction

The distribution and seasonal variance of water vapor in the stratosphere are still poorly understood. The significance of water vapor in stratospheric chemistry has been stressed by numerous investigators, including recently Hunt (1966), Hesstvedt (1968) and Hampson (1964[1]). They concluded that theoretically derived ozone distributions were more representative of distributions observed in the natural atmosphere if hydrogen-oxygen reactions were included in the model chemistry. Water vapor is a prime source of hydrogen.

Although worldwide samplings of tropospheric humidity to 8 km are made daily, routine synoptic study of the stratosphere has not been possible for lack of a relatively cheap, lightweight but accurate hygrometer. Such data as have been procured were obtained by bulky frost-point hygrometers and solar spectrometers flown to ~30 km on balloons by private investigators. In an effort to provide wider geographical and seasonal data coverage, the program to be described was inaugurated jointly by the Advanced Research Projects Agency, the U. S. Air Force, and the Defence Research Board of Canada.

A USAF aircraft was instrumented with an automatic tracking solar spectrometer and a magnetic tape recorder. The mobility and altitude capability of the aircraft were exploited to record repetitively solar spectra from 70N to 40S over North and South America. From the prominent absorption feature at 3854 cm^{-1} (2.59 μ), water vapor concentration was deduced. Other features, ascribed to ozone, nitrous oxide and carbon dioxide, were also prominent in the spectra, but they will be reported elsewhere. The immediate objective is to discuss the water vapor data secured during the first 13-month period of the trial program, April 1967 through May 1968.

[1] Private communication.

2. Equipment

A Perkin-Elmer 99G spectrometer was equipped with a 150 lines mm^{-1} grating, a cooled indium-antimonide detector and an electrically driven, self-reversing scan mechanism. The latter was set to scan a portion of adjacent grating orders, 2030–2420 and 3700–4000 cm^{-1}, as illustrated in the sample spectrum of Fig. 1. Extraneous grating orders were rejected by a 2.5–5.0 μ optical filter which was located immediately ahead of the entrance slit.

The spectrometer and solar tracker were housed in a pod which was attached to the leading edge of the right wing of the aircraft. Solar radiation entering the pod through a 10-inch diameter, 36-inch focal length arsenic trisulfide lens was deflected through 90° by a tracking mirror to a focus on the entrance slit of the spectrometer. Minor misalignment of the solar image on the slit was sensed by a quadrature array of tracking error detectors. Spectral resolution of 0.8 cm^{-1} at 3854 cm^{-1} was achieved with a 0.045-mm slit width.

Three additional mechanisms were incorporated to facilitate data evaluation and interpretation. Zero radiation, or dark condition, was simulated by insertion of an opaque shutter ahead of the entrance slit at one extremity of each spectral scan. Elsewhere in the scan, radiation intensity immediately aft of the entrance slit was measured by diverting a small fraction of the radiation passing through the slit to a rudimentary photom-

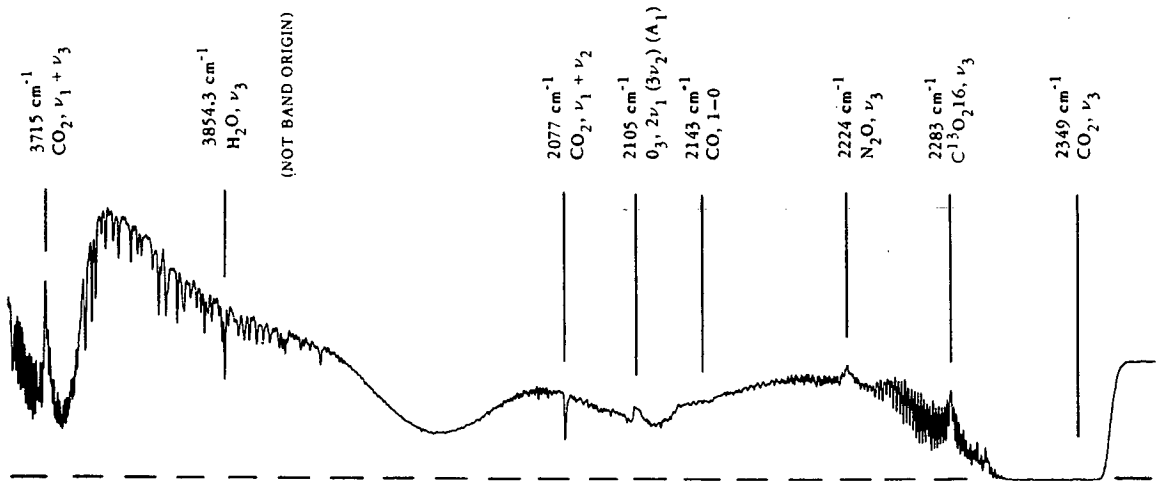

FIG. 1. Sample solar spectrum recorded from 17.7 km over New Mexico.

eter which was equipped with a narrow band 2.5 μ optical filter, a 133-Hz chopper, a lead sulfide detector, and appropriate electronics. Variation in radiation intensity through tracker misalignment or cloud obscuration resulted in variation of the lead sulfide detector output signal. By reference to this signal during initial inspection of recorded data, distortion of the 3854-cm^{-1} feature could be discovered and the affected spectra rejected. The 2.5 μ reference was chosen because atmospheric absorption was negligible at that wavelength for the range of solar elevations and aircraft altitudes experienced.

The third auxiliary mechanism consisted of a quartz-iodine lamp and lens, mounted such that the lamp's radiation traversed the same path in the pod as did the solar radiation. Lamp spectra were recorded at the beginning and end of each flight to verify the absence of contaminating water vapor. Free stream air was ducted through the apparatus to purge vapor outgassing from walls or which was trapped in poorly ventilated compartments. Residual water vapor would have produced discernible absorption at 3854 cm^{-1}; none was observed except on one occasion when the instrument operator was tardy in opening the purging control valve.

Direct current output signals were converted to frequency by voltage-controlled oscillators whose outputs were multiplexed and distributed over the seven tracks of the recorder. In addition to the solar spectrum, grating position, pressure altitude, and numerous monitoring parameters were recorded. Pressure altitude, derived from an excited potentiometer driven by the aircraft's aneroid altimeter, was estimated to be accurate to 0.09 km (300 ft). The solar spectrum, processed by a 500–12,000 Hz oscillator on an individual track, was linear to less than 1% over its dynamic range. Distortion from tape flutter and speed variations was reduced to less than 1% by compensation networks in the ground-based playback equipment.

3. Computational method

The computational method to be described is relevant to the reduction of any absorption feature where the absorption is by a unique species. For practical purposes, the absorption in the 3848–3860 cm^{-1} region of the solar spectrum can be regarded as unique to the ν_1 and ν_3 vibrational bands of water vapor. Overlapping by the adjacent CO_2 band centered at 3720 cm^{-1} is negligible. Gates *et al.* (1964) have listed the pertinent line parameters and Calfee and Gates (1966) have produced curves of growth for the 3848–3860 cm^{-1} feature. They assumed Lorentzian line shapes at all pressures, and uniform mixing from the upper troposphere to the top of the atmosphere. This interval was divided into 8 layers of equal pressure differential, and each layer was assigned a temperature conforming to the *U. S. Standard Atmosphere, 1962*, at mid-latitudes. Their curves of growth were used throughout the program because, although of theoretical origin and ignoring Doppler effects at low pressures, they were judged to be more tractable and at least as accurate as the sparse absorption cell data available at the time.

After each flight, a small digital computer calculated the absorption at 3848–3860 cm^{-1} for each spectrum directly from the magnetic tape in real time. Spectral limits were recognized by reference to a pulse train generated by the grating drive mechanism. The apparent zero absorption level, or "solar envelope," was determined by sampling the amplitude of the two shoulders bordering 3848 and 3860 cm^{-1} as shown in Fig. 2. The continuum at each shoulder resulting from overlapping of the extreme wings of strong water vapor lines was evaluated from the absorption experienced during each scan and was added to the shoulder before calculation of the final cumulative absorption integral. Continuum contribution varied from 0.5–5% for the range of conditions met. Zero radiation was established by reference

to the completely opaque region at 4.3 μ which is ascribed to absorption by the ν_3 band of CO_2.

The measured absorptances were converted to slant-path water vapor abundances by reference to the Calfee and Gates (1966) curves of growth. An empirical fit [Eq. (1)] was applied to allow interpolation over the range of pressures and abundances experienced. Coefficients were selected such that pressure P represented the pressure altitude in millibars at the instrument and $\int A(\nu)d\nu$ was the cumulative absorption integral in wavenumbers for the 3848–3860 cm^{-1} interval. The precipitable centimeters w of water vapor, calculated for the slant path, is lower by 3% or less than the Calfee and Gates values for small absorptances (0.8 cm^{-1}) and higher by 1.5% for large absorptances (5 cm^{-1}) at all pressures from 50–243 mb. These errors in empirical fit were judged to be acceptable since the Calfee and Gates calculation of abundance in a uniformly mixing atmosphere is regarded as accurate to within but ±25%. The equation used for w was as follows:

$$w=\frac{\log_e^2(1-A/12)}{P}(4.82-B), \quad (1)$$

where A is the cumulative absorption integral, 3848–3860 cm^{-1}, in wavenumbers, and

$$B=(1.82+0.0051P)(A+0.652-0.005008P)\times\exp[-A(0.655-0.00155P)]. \quad (2)$$

The slant path abundance w was converted to mass mixing ratio from the instrument to the top of the atmosphere (assuming uniformity), using the expression

$$r(1,0)=wg/(PN), \quad (2)$$

where g is the gravitational acceleration constant, P the pressure in millibars at instrument altitude, and N the equivalent air mass in the slant path. The Bemporad (see List, 1951) tables, defining the zenith distance as unity air mass, were used to calculate N from a least-squares fit of the instrument operator's observations of solar zenith angle, accurate to ±0.5°. Data where zenith angles >85° (10 air masses) were rejected to reduce computational uncertainty.

The most significant computational uncertainties stemmed from the Calfee and Gates estimate of slant path water vapor abundance as a function of cumulative absorption, the assumption of uniform mixing above the instrument, and the use of Lorentz-shaped lines at all pressures. From the recent frost-point hygrometer measurements of Mastenbrook (1968) and Sissenwine *et al.* (1968), uniform mixing appears realistic for at least the first scale height above the highest aircraft altitude. A Voigt profile for line shapes, embodying Doppler effects at low pressures, would have been preferable to the Lorentz profile. Unfortunately, the Voigt profile, or an adequate simulation of it, had not been incorporated into a suitable computer program at the time of data processing. Selected data may be treated again at some future date to assess the improvement achieved from use of the Voigt profile.

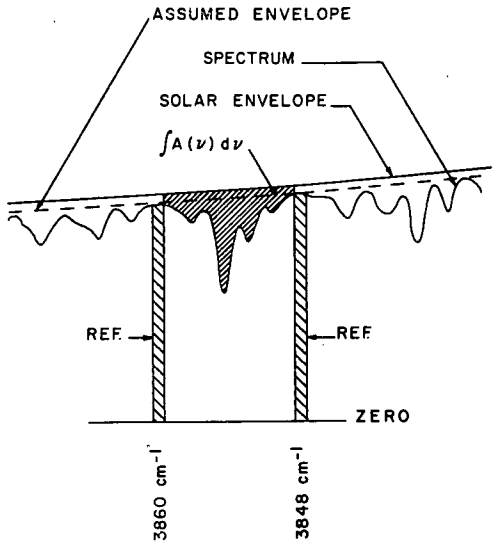

FIG. 2. Sample recording of 3848–3860 cm^{-1} region and associated solar envelope.

Mixing ratios from fixed altitude flights were smoothed numerically by a Gaussian function with a half-width equivalent to five consecutive spectral intervals (equivalent to approximately 15 n mi in still air) before plotting as a function of geographical position. Vertical distributions measured during aircraft ascent or descent were computed by converting each absorption integral to slant path abundance, normalizing to zenith conditions, smoothing, differentiating the smoothed abundance with respect to altitude, and finally converting the differentials to ambient mixing ratios. Zenith abundances were smoothed numerically by a Gaussian function of 0.5 km half-width before differentiation. Ambient mixing ratios were tabulated at 0.25-km intervals.

4. Results

The basic goal of the water vapor measurement schedule was to evaluate stratospheric concentrations at regular intervals from 70N to 40S for at least one calendar year and preferably for two years. The data reported herein were obtained during the first 13 months of the schedule; additional measurements are scheduled to follow, although at a less frequent rate.

Two basic flight patterns were employed throughout the trials. Ambient concentrations in the upper troposphere and lower stratosphere were deduced from solar spectra recorded while ascending or descending slowly. Ascent and descent usually commenced over a single geographical location on each flight so as to confine the two tracks to approximately the same general air mass.

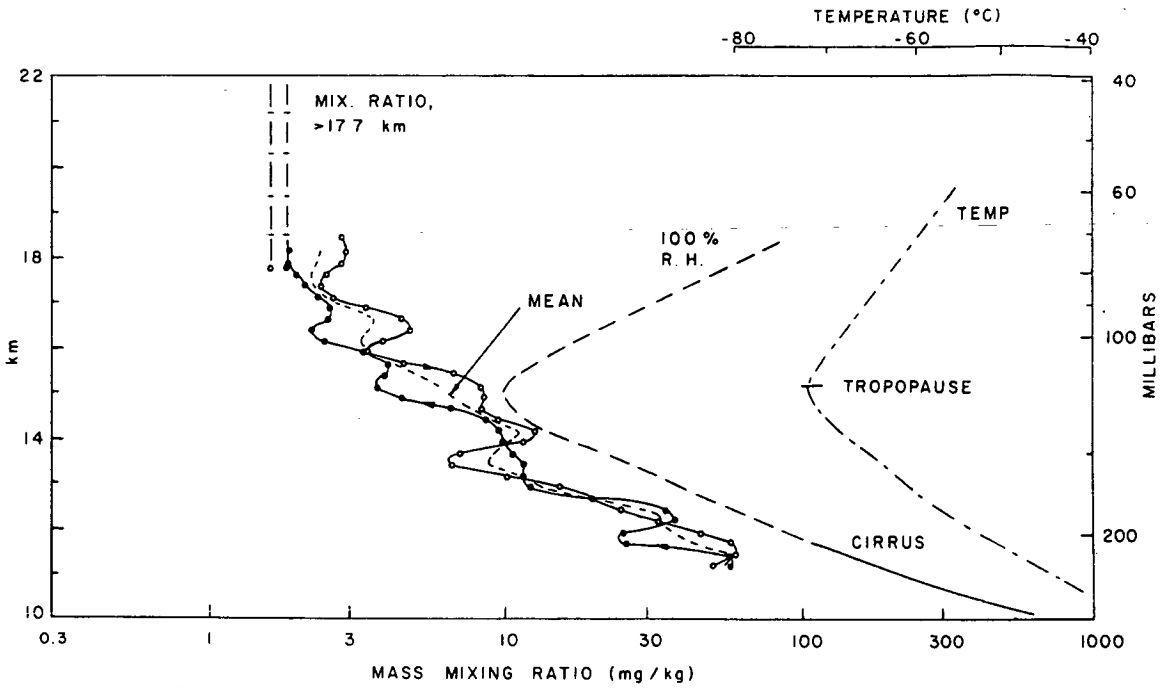

FIG. 3. Water vapor mixing ratio distribution with height above Colorado–New Mexico, 8 August 1967.

Pressure altitude limits were habitually 10.7 (35,000 ft) and 18.3 (60,000 ft) km except in Alaska where 7 km was used as a base to ensure tropopause penetration. Latitudinal distributions were traced by maintaining a fixed altitude of 17.7 km along a generally north-to-south track while recording spectra of the setting sun. Minor deviations of about ±1 km were introduced at the beginning, middle and end of each recording to sample the ambient concentrations at 17.7 km at three points along the track.

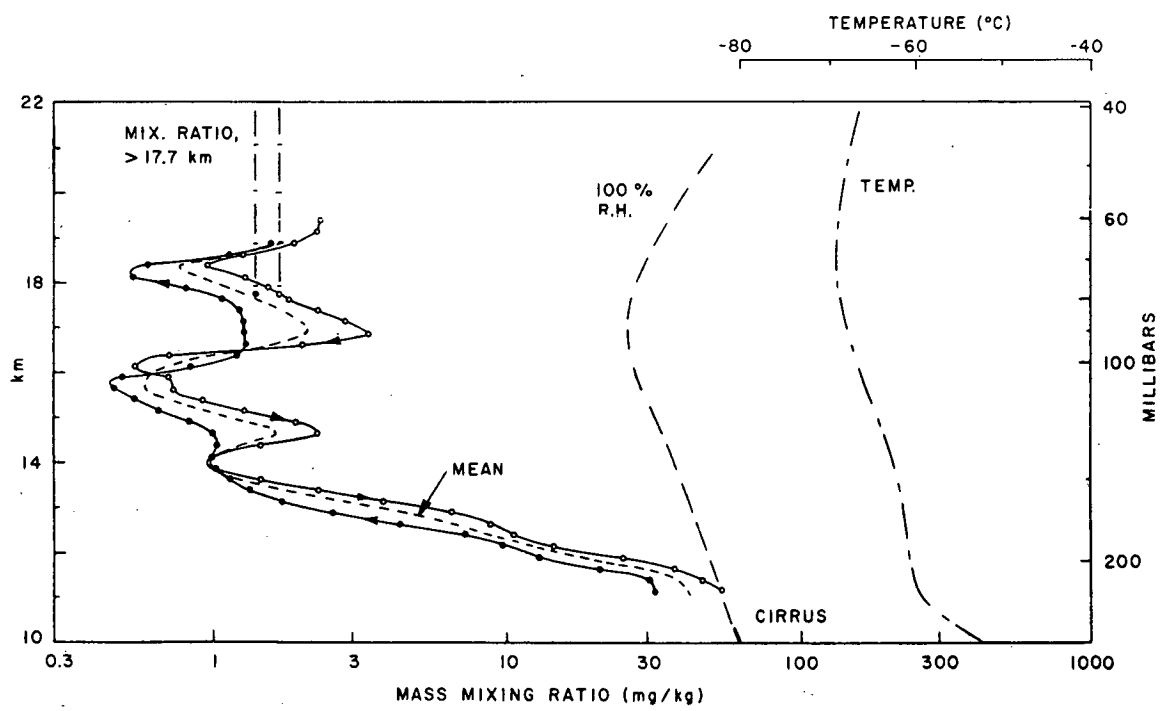

FIG. 4. Water vapor mixing ratio distribution with height above Colorado–New Mexico, 23 December 1967.

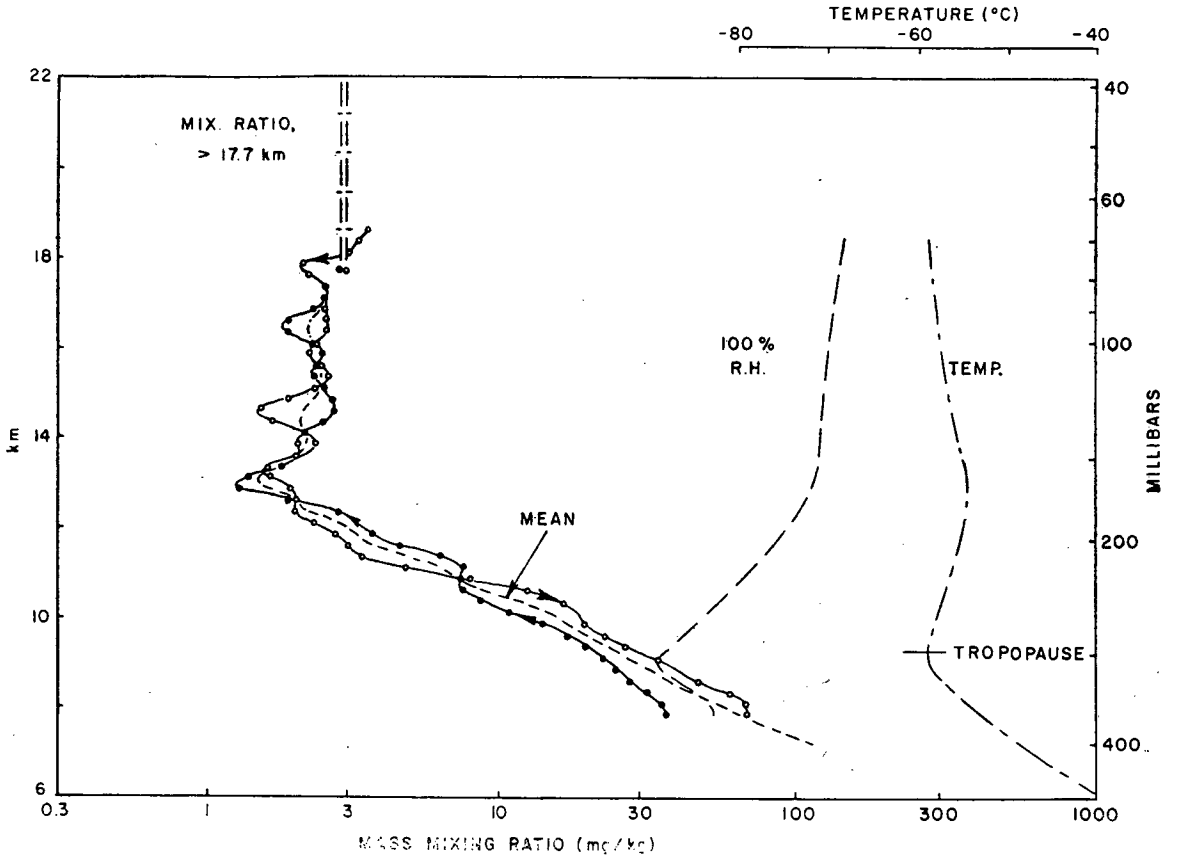

FIG. 5. Water vapor mixing ratio distribution with height above Alaska, 25 March 1968.

Most of the flights were conducted within ±18° latitude of Albuquerque, N. M., the maximum deployment allowed by tape recorder capacity for a single return flight. Flights to the north and south of Albuquerque for latitudinal coverage were scheduled on consecutive days when possible so as to reduce potential discontinuities in the water vapor profile due to evolution of the air mass. Distribution with altitude in the Colorado–New Mexico area was measured approximately thrice monthly with as near equal spacing between flights as possible. Both flight patterns were utilized during aircraft deployment for short periods to Alaska in January and March 1968 and to the Panama Canal Zone and Argentina in January 1968.

The distributions over the Colorado–New Mexico area showed a characteristic decline in concentration with altitude to some 2 km above the tropopause and relatively uniform mixing immediately beyond that altitude to 18.5 km. Distributions representative of summer and winter conditions are shown in Figs. 3 and 4. Temperature profiles, constructed from routine rawinsonde data obtained at the time and locale nearest the event, are also shown. The tropopause height denoted in each case represents the lowest altitude at which a pronounced change in temperature gradient was observed; it may not be in precise agreement with that published by the various weather services. In summer, the stratospheric temperature profile approached equatorial conditions, whereas in winter, when the jet stream moved southward of Colorado–New Mexico, the vertical profile was characteristic of the mid-latitudes as defined by the *U. S. Standard Atmosphere, 1962*.

The drying trend with altitude in the 2-km layer immediately above the tropopause is evident in both summer and winter profiles. Although vertical motion is effectively "capped" by the temperature discontinuity at the tropopause, water vapor obviously penetrates this barrier, probably through eddy diffusion (Manabe *et al.*, 1965). Below the tropopause, mixing ratios at 12 km were observed to be 4–8 times higher in summer than in winter. The mean mixing ratios for the atmosphere above 19 km, assuming uniform mixing to the top of the atmosphere, were observed to vary by only a few per cent seasonally.

Comparison of the measured profile with the mixing ratio profile for 100% relative humidity provided a crude check on the validity of the computational technique and on the accuracy of the measurement.

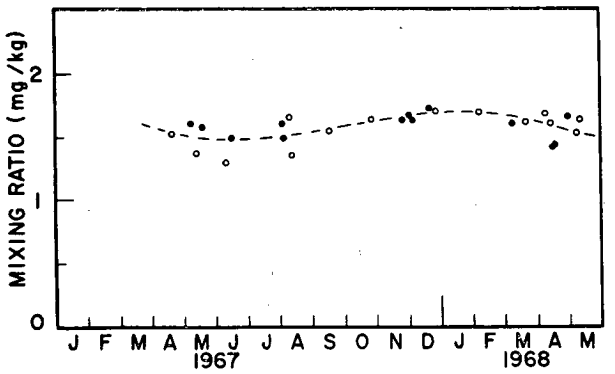

FIG. 6. Mass mixing ratio of water vapor above 17.7 km at 37N, 108W: average of 20 spectra while at 17.7 km, level flight, solid circles; average of 10 spectra while ascending or descending through 17.7 km, open circles; monthly mean, dashed line.

Thus, if scattered clouds were reported at the lowest altitude, an ambient mixing ratio corresponding to 50% or higher relative humidity was anticipated. The instrument could not function in cloud as a clear view of the sun was required. Cirrus cloud, embedded in haze, was reported for each of the August and December flights. The cloud layer is delineated by the solid portion of the 100% relative humidity curves of Figs. 3 and 4. Extrapolation of the mean ambient mixing ratio profile to cloud top height in each case infers a relative humidity in excess of 40% on 8 August and 80% on 23 December. A similar plot for 25 March over Alaska (Fig. 5) indicates 100% relative humidity at the tropopause, although cloud was not reported in the flight log. As to whether this was an oversight or that none was observed is uncertain. While not a rigorous check of accuracy, it can be accepted from this comparison that ambient mixing ratios in the troposphere are accurate at least to ±50%.

Ambient mixing ratio trends during ascent and descent correlated in gross detail. The data from Figs. 3–5 illustrate sample variance. Unfortunately, the measurements could not be taken simultaneously. Measurement duration approximated 3 hr, and the starting and finishing points for each ascent and descent were separated in a generally north-south direction by 250–300 n mi. Thus, any inhomogeneities in composition induced by atmospheric circulation and by latitudinal displacement were reflected in the observations.

Evidence of stratification immediately above the tropopause was observed on some flights. Height correlation in the December vertical distribution over Colorado–New Mexico of Fig. 4 was good, although it was more exact than experienced generally. The factor of 6 variability in the stratosphere of Fig. 4 may be exaggerated by a factor of 2. Uncertainties are highest when computing the drier concentrations by differentiation. Ambient concentrations >2 ppm are estimated as accurate to ±50%, but only to a factor of 2 below a calculated 1 ppm.

If the variability in the ambient from 14–18 km of Fig. 4 is ignored and a mean ambient taken, this mean is 1.3 ppm, slightly drier than the 1.5 ppm calculated for the atmosphere above 17.7 km where uniform mixing to the top of the atmosphere was assumed. This trend conforms to winter and spring vertical distributions measured for that geographical area. Mean ambient mixing ratios were lowest ~2 km above the tropopause, and they increased in the next 3–5 km to values consistent with the vertical mean above 17.7 km.

Mixing ratios above 17.7 km over Colorado–New Mexico, calculated assuming uniform mixing to the top of the atmosphere, were relatively stable with season. Fig. 6 contains a plot of mixing ratios measured within a 100-mi radius of 37N, 108W. The open circles represent data obtained while the aircraft was ascending or descending through 17.7 km, ~10 consecutive spectra being averaged per point. The solid circles are the average of approximately 20 spectra obtained while

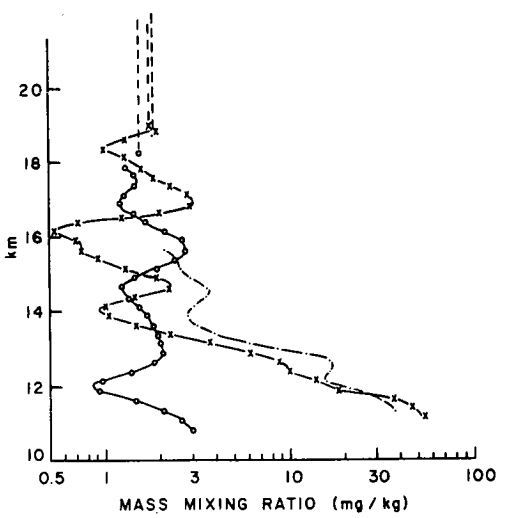

FIG. 7. Comparison of water vapor distribution with height over North America during the northern winter: Alaska, 65N, 23 January 1968, open circles; New Mexico, 38N, 23 December 1968, crosses; Panama, 7 January 1968, dots; respective concentrations to the top of the atmosphere, dashed lines.

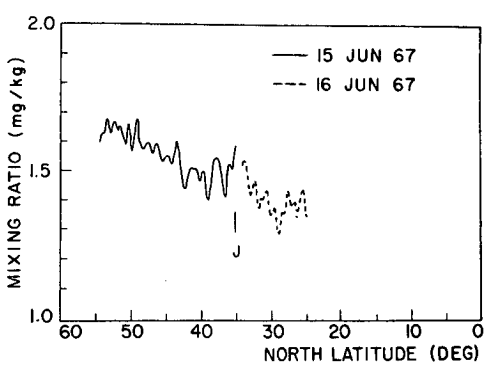

FIG. 8. Water vapor concentration above 17.7 km as a function of latitude, June 1967.

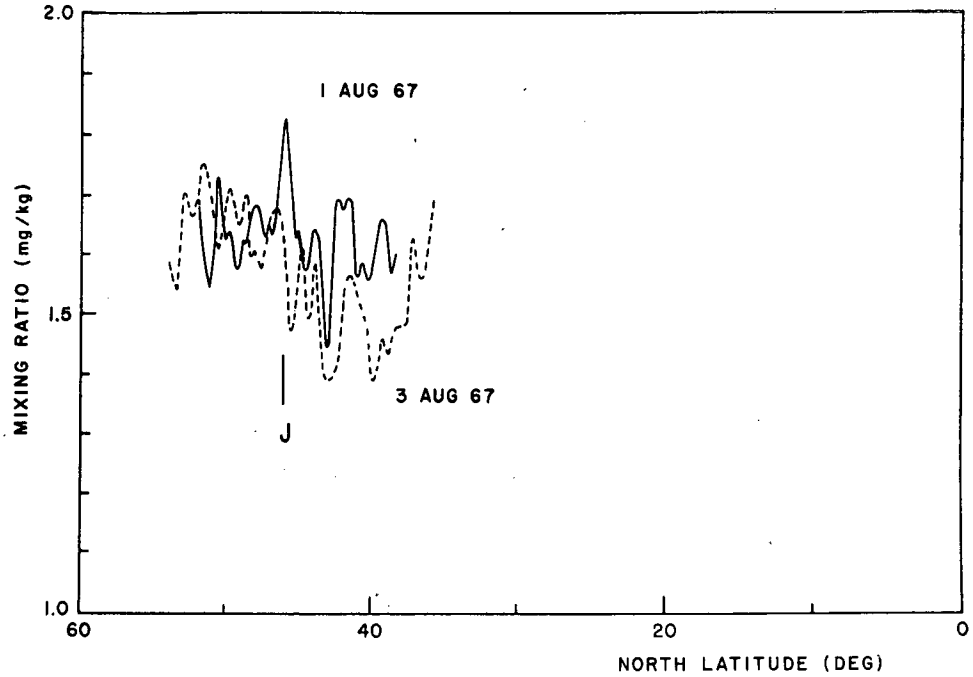

FIG. 9. Water vapor concentration above 17.7 km as a function of latitude, August 1967.

passing 37N at a 17.7-km altitude. The monthly median, delineated by a broken line, infers a seasonal low of 1.45×10^{-6} in June 1967 and a high of 1.7×10^{-6} in January 1968, a seasonal change of 17%. The percentage scatter from the median is of the same order. Approximately half the scatter can be charged to instrumental sources, but the remainder is regarded as of atmospheric origin.

Comparison of sample ambient mixing ratio distributions over Alaska, New Mexico, and the Panama Canal Zone for northern midwinter is made in Fig. 7. Only the mean of the ascending and descending distributions is shown. The mixing ratio at 12 km was an order of magnitude higher at the two southern sites than in Alaska where the tropopause height was <10 km. At 16 km, ambient mixing ratios at all sites approximated 1.7 mg kg^{-1} if the variation induced by strata was removed by averaging. The concentrations above 17.7 km to the top of the atmosphere differed only slightly (6% for these three samples).

Latitudinal distributions of water vapor above 17.7 km were sampled at all seasons between 53N and 20N, but were only traced during the northern winter over Alaska and to the south of 20N because of the diffi-

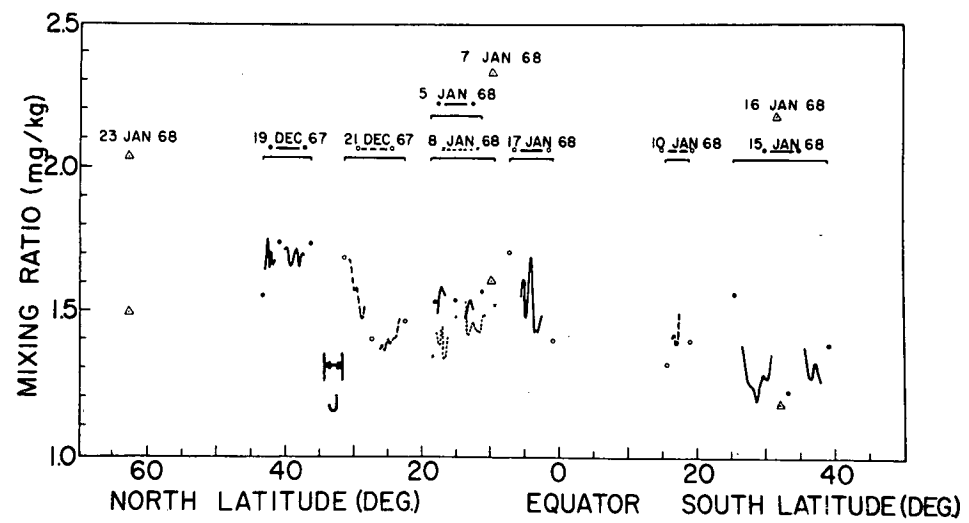

FIG. 10. Water vapor concentration above 17.7 km, December 1967–January 1968.

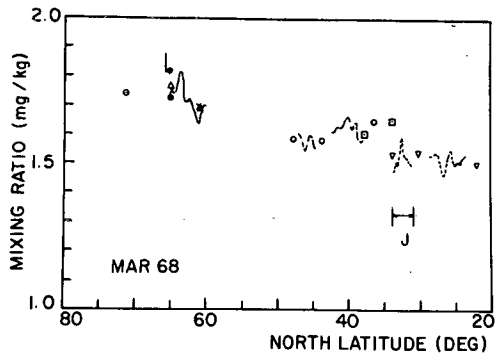

FIG. 11. Water vapor concentration above 17.7 km, March 1968.

culties associated with deployment of the aircraft to operating bases remote from New Mexico. Profiles traced are shown in Figs. 8–12 for June, August, December–January, March and April–May. As previously described, uniform mixing to the top of the atmosphere was assumed. Data were smoothed numerically by applying a Gaussian function with a half-width of 5 consecutive spectra (~15 n mi travel under calm conditions). Lines and individual points represent data taken from a constant altitude of 17.7 km and as the aircraft passed through 17.7 km, respectively.

As stated previously, the segment 20–53N was sampled more frequently than the remaining latitudes. Each profile traced in this segment indicated declining mixing ratios with decreasing latitude, regardless of season. Seasonal effects, although probably present, were so small that they were masked by the scatter in the data. The median of 1.64×10^{-6} for all data at 50N declined to 1.46×10^{-6} at 25N, i.e., by 11%.

The mean mixing ratios above 17.7 km, plus upper and lower limits delineating the extremes observed, are plotted in Fig. 13 as a function of latitude for all data acquired during the 13-month test period without regard to season. Unfortunately, the seasonal weighting is inadequate for firm conclusions on seasonal effects to be drawn. The extreme north, equatorial and south latitudes were sampled only in the January–March period, whereas the 20–53N segment was sampled at all seasons. The latter segment did not show pronounced seasonal variance and it is felt that one can assume that the profile of Fig. 13 is representative of January–March conditions for 1968.

It was desirable to produce latitudinal coverage along one meridian of longitude, but this was not possible because of the necessity to track the sun and occasionally because of restrictions to allotted air space. Thus, tracks immediately to the north of New Mexico followed the eastern slopes of the Rocky Mountain chain whereas those to the south were displaced eastward to cross the Gulf of Mexico along a line joining Louisiana and Panama. To determine if this lateral displacement introduced a significant discontinuity in the concentration profile, the spectrometer was flown at 17.7 km approximately along the 35th parallel of latitude eastward at noon on 30 November 1967 from New Mexico to Alabama. The median concentration above 17.7 km declined linearly from 1.65 mg kg^{-1} at 105W to 1.58 mg kg^{-1} at 87W, a drop of 4.2%. This decline could not be charged to progressive drying of a

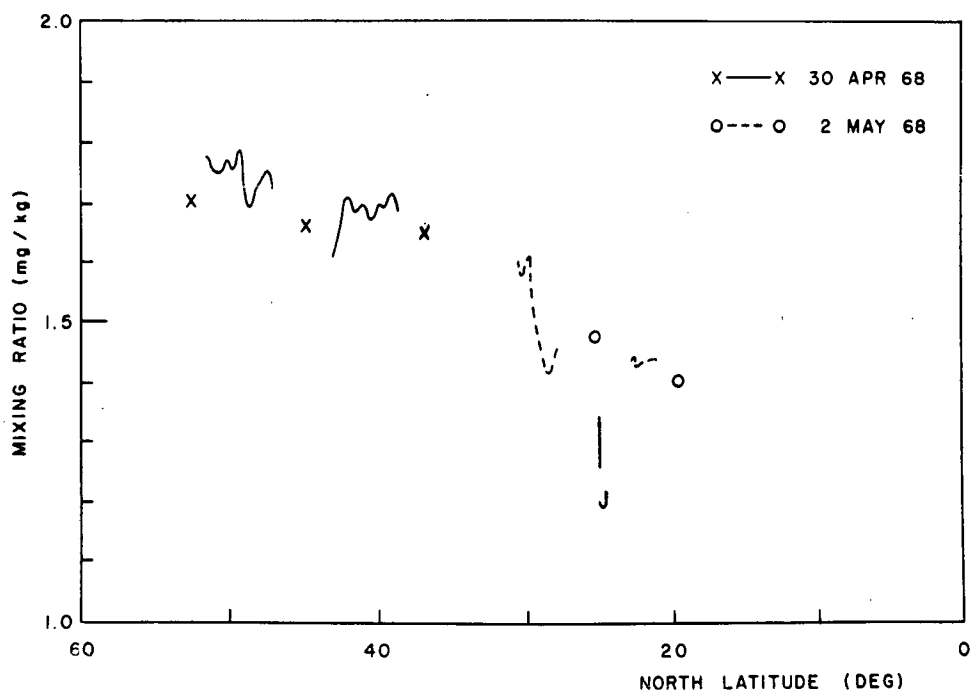

FIG. 12. Water vapor concentration above 17.7 km, April–May 1968.

contaminated instrument as the initial lamp spectra were free of absorption at 3854 cm^{-1}. Thus, for this single measurement, no gross variation was experienced with longitude across southern continental United States.

Tracks over Alaska were also displaced longitudinally from those to the east of the Rocky Mountains. West-to-east flights were conducted on 23 January and 22 March 1968 over southern Alaska and along the northern coast of the Northwest Territories, respectively. Over Alaska, the median of water vapor concentrations above 17.7 km, assuming uniform mixing, increased from 1.46 mg kg^{-1} at 61N, 161W to 1.62 mg kg^{-1} at 63N, 148W, a reversal of the trend over southern United States and a larger change in a somewhat shorter distance. The March flight along the northern coast of the Northwest Territories produced similar results. The median increased slightly from 1.72 mg kg^{-1} at 71N, 135W to 1.77 mg kg^{-1} at 69N, 103W.

The latitude at which the subtropical jet stream intersected the aircraft's track is indicated in Figs. 8–12 by J. Characteristically, this high velocity stream of air approaches North America from the North Pacific Ocean near the Canadian–United States border, is diverted southward across southern United States or northern Mexico, and finally leaves North America on a northeastward course for the Atlantic Ocean. During northern winter and spring, the segment of concern is situated at or near 25–30N and the core speed exceeds 100 kt. It migrates northward to 40–45N in summer and the speed slows to less than 100 kt. The northern edge of the core delineates a break in the tropopause through which stratospheric air sinks into the troposphere. No pronounced variation in water vapor concentration near this break was discerned from an altitude of 17.7 km, a result which would be anticipated if mixing in the lower stratosphere is nearly uniform with height.

5. Discussion

Solar spectra were recorded over North and South America from a high flying aircraft during April 1967–May 1968. An atmospheric absorption feature at 3854 cm^{-1} was used to deduce the mean mixing ratio of water vapor to air above the aircraft to the top of the atmosphere at a variety of latitudes and in different seasons. Ambient water vapor mixing ratios were deduced also by differentiation of the 3854 cm^{-1} absorption recorded while the aircraft ascended or descended between 10.7 and 18.3 km.

Computation of the mean mixing ratio above the aircraft when flying at constant pressure altitude assumed uniform mixing from aircraft altitude to the top of the atmosphere. Flights at a fixed pressure altitude of 17.7 km during the winter and spring of 1967–68 along north–south and west–east tracks showed that the

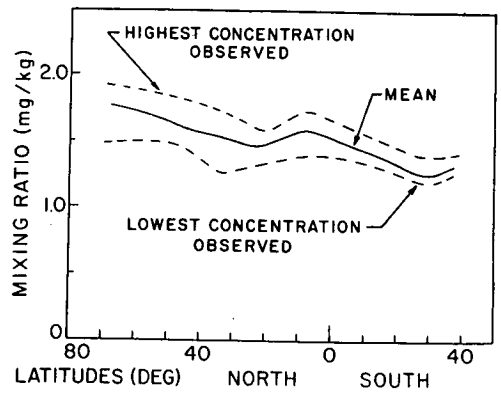

FIG. 13. Mean water vapor concentration above 17.7 km over North and South America, Northern Hemispheric winter.

median of the mean mixing ratio varied with latitude and with longitude. The winter and spring median declined from 1.75 mg kg^{-1} at 65N to 1.25 mg kg^{-1} at 30S with an intermediate minimum and maximum of 1.45 and 1.6 mg kg^{-1} at 25N and 7N, respectively. Three similar flights of approximately 1000 mi each along west-to-east tracks indicated an increase in the median from 1.46–1.62 mg kg^{-1} across southwestern Alaska in January and a smaller increase from 1.72–1.77 mg kg^{-1} with eastward passage along the seventieth parallel over northwestern Canada. Conversely, a slight decline from 1.65–1.58 mg kg^{-1} was observed along a track between New Mexico and Albama in November. All of these concentrations represent relative humidities of a few per cent. The stratosphere above 17.7 km was therefore very dry everywhere, and differences in concentration between polar and equatorial regions were relatively small.

Ambient mixing ratios in the altitude region 10.7–18.3 km declined with altitude from 10.7 km to a height approximately 2 km above the tropopause. In general, minimum ratios were observed at the latter height. Where this height was lower than 18.3 km, the median of the ambient ratios increased with altitude to 18.3 km by factors of 1–2 in general to approach the 1.4–1.7 mg kg^{-1} observed as median ratios seasonally in that portion of the atmosphere from 17.7 km to the top (uniform mixing was assumed in the latter region). Significant modulation of the ambient mixing ratio profiles was observed at altitudes just below 18.3 km. Height correlation of maximum and minimum ratios on ascending and descending tracks of some flights was sufficient to indicate the presence of stratified layers in the lower stratosphere.

Ambient mixing ratios over Colorado–New Mexico varied significantly with season at altitudes <17.7 km. Ambient ratios at 12 km were highest in August (no observations were made in July) and lowest during winter and spring. August concentrations exceeded those of winter by factors of 4–8. This magnitude decreased

with height above 12 km to a few per cent at 17.7 km. The monthly mean mixing ratios above 17.7 km, assuming uniform mixing to the top of the atmosphere, fluctuated seasonally from 1.45 mg kg^{-1} in June to 1.7 mg kg^{-1} in January. This observed cyclic variation above 17.7 km in the Colorado–New Mexico area was out of phase with the variation in ambient mixing ratios below 17.7 km where highest and lowest concentrations were recorded in summer and winter, respectively. A similar phase relationship was observed in 1965–66 in the ambient concentration in the lower stratosphere and upper troposphere over California by Sissenwine *et al.* (1968), using a balloonborne frost-point hygrometer. Investigation of the responsible transport mechanism will not be pursued in this text.

Determination of the seasonal variation in the mean mixing ratio above 17.7 km at latitudes remote from New Mexico was not possible because of lack of seasonal coverage. Measurements were representative of northern winter and spring conditions, except in the latitude segment 35–53N which was covered in summer as well as winter and spring. Seasonal variation was sufficiently small at the northern extremity of this segment, 45–50N, that it could not be distinguished from the combined instrumental noise and small-scale atmospheric variability experienced on the six flights concerned. After smoothing data numerically with a Gaussian function of half-width equal to 5 consecutive spectra (approximately 15 n mi), the resultant maximum dispersion was less than 15% from the median for all flights.

The mean mixing ratio of 1.6 mg kg^{-1} above 17.7 km measured at 7N on 17 January 1968 (Fig. 13) agrees with the hypothesis that the equatorial tropopause temperature controls stratospheric humidity. Thus, water vapor diffusing upward from the warm, moist equatorial troposphere will condense and precipitate back into the troposphere as it enters the cold layer associated with the equatorial tropopause. The concentration of that which diffuses upward across this layer is limited by the saturation vapor pressure for the coldest temperature, nominally −80 to −85C. The rawinsonde temperature minimum associated with the flight across 7N was −84.1C at 79 mb, corresponding to a saturation mixing ratio of 2.16 mg kg^{-1}. Ten days earlier, a temperature of −85.1C at 92 mb, corresponding to 1.52 mg kg^{-1}, was reported. Thus, the concentrations observed at all latitudes are within a few per cent of the limiting concentration at the equatorial tropopause.

Mean mixing ratios calculated for the atmosphere above 17.7 km are by the nature of the measurement most representative of concentrations in the next scale height, this is from 17.7–24 km. The 1.45–1.7 mg kg^{-1} median of Fig. 6, observed over Colorado–New Mexico (38N), was in reasonable agreement with Mastenbrook's frost-point hygrometer observations over Washington, D. C. (39N), in 1964–65. Median values of ambient concentration for the two-year period varied from 2.2 mg kg^{-1} at 80 mb (17.7 km) to 2.5 mg kg^{-1} at 25 mb (25 km). The approximate discrepancy of 30% probably arises from instrumental uncertainties; our data cannot accommodate 30% variation over such a distance along a common latitude. Great care was taken in both sets of observations to suppress contamination by water vapor of surface origin. The solar spectrometric data were judged to be free of contamination as spectra recorded in flight using the tungsten lamp as a radiation source contained no water vapor absorption features. The curves of growth employed to convert absorptance at 3854 cm^{-1} to abundance were estimated to be accurate to only ±25%.

The winter–spring distribution with latitude of mean mixing ratios above 17.7 km shown in Fig. 13 agrees qualitatively with that computed by Manabe *et al.* (1965) in preparing their numerical model of atmospheric circulation. Concentrations observed at high latitudes were greater than at low latitudes, as predicted, but the magnitude of the predicted change was larger than observed. The discrepancy would appear to be at the high latitudes where the model predicts higher ambient mixing ratios in the lower stratosphere than observed. For example, at 65N the predicted ambient at 15 km is 7 mg kg^{-1}, whereas our measurements over Alaska in January and March show ~1.5 mg kg^{-1}. The model also predicts declining mixing ratios with increasing altitude to 30 km. Our Alaskan measurements show ambient concentrations to be lowest just above the tropopause and to increase slightly in the next 5 km as per Fig. 5. Thus, one must conclude that the actual atmosphere was drier and more uniformly mixed than predicted at high latitudes, giving rise to the smaller variation in the observed mean mixing ratios above 17.7 km with latitude.

The profile of Fig. 13 shows concentrations near 25N and in the southern latitudes which are slightly lower than that over the equator, which is presumed to be the control zone. Data treatment was identical to that for other latitudes: instrumental flaws were investigated but none were uncovered. These exceptional concentrations, especially the lowest ones in the Southern Hemisphere, suggest that the hypothesis of water vapor removal at the equatorial tropopause may not adequately explain stratospheric water vapor control at all latitudes. Further measurements are planned to verify the data from the Southern Hemisphere.

Acknowledgments. The authors wish to thank the U. S. Air Force and the Advanced Research Projects Agency for conducting the flight program. They are indebted especially to Mr. P. Nutting of ARPA and to the crews who flew the aircraft.

Mention must be made also of the efforts of Dr. R. P. Lowe and Mr. R. Lafrance who devised the computer programs, and of the Computing Devices of Canada

field team which serviced and maintained the aircraft's instrumentation. Mr. J. Hampson and Dr. C. Cumming were extremely helpful in discussion and they supplied numerous suggestions and constructive criticisms.

REFERENCES

Calfee, R. F., and D. M. Gates, 1966: Calculated slant-path absorption and distribution of stratospheric water vapor. *J. Appl. Opt.*, **5**, 287–292.

Gates, D. M., R. F. Calfee, D. W. Hansen and W. S. Benedict, 1964: Line parameters and computed spectra for water vapor bands at 2.7 μ. Natl. Bur. Stands, Monogr. 71, Washington, D. C., Govt. Printing Office, 126 pp.

Hesstvedt, E., 1968: On the effect of vertical eddy transport on atmospheric composition in the mesosphere and lower thermosphere. *Geofys. Publikasjoner*, **27**, 1–35.

Hunt, B. G., 1966: Photochemistry of ozone in a moist atmosphere. *J. Geophys. Res.*, **71**, 1385–1398.

List, R. J., 1951: *Smithsonian Meteorological Tables*, 6th rev. ed. Washington, D. C., Smithsonian Institute, p. 422.

Manabe, S., J. Smagorinsky and R. F. Strickler, 1965: Simulated climatology of a general circulation model with a hydrologic cycle. *Mon. Wea. Rev.*, **93**, 769–798.

Mastenbrook, H. J., 1968: Water vapor distribution in the stratosphere and high troposphere. *J. Atmos. Sci.*, **25**, 299–311.

Sissenwine, N., D. D. Grantham and H. A. Salmela, 1968: Midlatitude humidity to 32 km. *J. Atmos. Sci.*, **25**, 1129–1140.

United States Committee on Extension to the Standard Atmosphere, 1962: *U. S. Standard Atmosphere, 1962*, Washington, D. C., Govt. Printing Offices, 278 pp.

88 WMS 1-7-1970 #6819

3-DSIS
Plus dist.

done
- 1-Ref file
- 1-Microfiche
- 1-DREP
- 1-CRC
- 1-DREA
- 1-SSO